nature astronomy

SUPPLEMENTARY INFORMATION

https://doi.org/10.1038/s41550-020-1120-5

In the format provided by the authors and unedited.

Resonance locking in giant planets indicated by the rapid orbital expansion of Titan

Valéry Lainey[1,2]✉, Luis Gomez Casajus[3], Jim Fuller[4], Marco Zannoni[3], Paolo Tortora[3], Nicholas Cooper[5], Carl Murray[5], Dario Modenini[3], Ryan S. Park[1], Vincent Robert[2,6] and Qingfeng Zhang[7]

[1]Jet Propulsion Laboratory, California Institute of Technology, Pasadena, CA, USA. [2]IMCCE, Observatoire de Paris, PSL Research University, CNRS, Sorbonne Université, Paris, France. [3]Dipartimento di Ingegneria Industriale, Università di Bologna, Forlì, Italy. [4]TAPIR, California Institute of Technology, Pasadena, CA, USA. [5]Queen Mary University of London, London, UK. [6]IPSA, Ivry-sur-Seine, France. [7]Department of Computer Science, Jinan University, Guangzhou, P R China. ✉e-mail: lainey@imcce.fr

Resonance locking in giant planets indicated by the rapid orbital expansion of Titan

-Supplementary Information-

Valéry Lainey[1,2*], Luis Gomez Casajus[3], Jim Fuller[4], Marco Zannoni[3], Paolo Tortora[3], Nicholas Cooper[5], Carl Murray[5], Dario Modenini[3], Ryan Park[1], Vincent Robert[2,6], Qingfeng Zhang[7]

[1]Jet Propulsion Laboratory, California Institute of Technology,

4800 Oak Grove Drive, Pasadena, CA 91109-8099, United States

[2]IMCCE, Observatoire de Paris, PSL Research University, CNRS,

Sorbonne Universités, UPMC Univ. Paris 06, Univ. Lille, 77

[3]Dipartimento di Ingegneria Industriale, Università di Bologna, 47121 Forlì, Italy

[4]TAPIR, Mailcode 350-17, California Institute of Technology, Pasadena, CA 91125, USA

[5]Queen Mary University of London, Mile End Rd, London E1 4NS, United Kingdom

[6]IPSA, 63 bis boulevard de Brandebourg, 94200 Ivry-sur-Seine, France

[7]Department of Computer Science, Jinan University, Guangzhou 510632, P. R. China

[*]To whom correspondence should be addressed; E-mail: lainey@imcce.fr.

Computing Q values In Table 1, we list the Q of Saturn corresponding to the values of $Im(k_2)$ in Table 1 in the main text, assuming a fixed $Re(k_2) = 0.382$. These Q values correspond to those shown in Figure 1 of the main text. Because of the non-linear relations between the variables, to correctly compute Q and its uncertainty we used a Monte Carlo approach. For each estimation of $Im(k_2)$, we generated a white Gaussian random vector, with mean and standard deviation equal to the estimated value and uncertainty (1σ), respectively. Then, we computed the vector of Q using the full, non-linear expression, obtaining a non-Gaussian distribution. The provided central value is the mean of the obtained random vector, while the given uncertainties are the 0.15 and 99.85 percentile, which correspond to the a 3σ confidence interval of a Gaussian distribution. For Mimas, the uncertainty of $Im(k_2)$, estimated using the astrometric approach, was similar to the value itself. Hence, some elements of the generated random vector of Q are negative, which represent a non-physical negative dissipation. For this reason, the negative values were discarded when computing the mean value of Q and the associated uncertainty. In any case, the uncertainty of Saturn's dissipation at Mimas's frequency is too large to make robust conclusions. For Enceladus and Dione, the assumed heating rate affects in a non negligible way the estimated values of $Im(k_2)$. In these cases, in Table 1 we provide the total mean and the global confidence level of Q, considering the minimum and the maximum expected heating rates.

Statistical Fit to Models Here we statistically quantify the statement that a tidal migration model with constant $t_{\rm tide}$ is more likely than a model with constant Q. To do so, we perform a least squares fit to the data for a model with an identical value of $Im(k_2) = -k_2/Q$ for each moon, i.e., a model with constant Q for Saturn at each moon's frequency. We fit to the values shown in Table 1 of the main text, using $k_2 = 0.382$. For Titan, we use the value of $Im(k_2)$ from radio tracking data because of its smaller uncertainty. We perform this fit for each value of

Supplementary Table 1: **Derivation of tidal Q parameter.** Similar to the table of k_2 values in the main text, but now converted into Saturn's effective values of Q shown in Figures 1 and 2 of the main text. The Q values are measured from the first set of orbital simulations as described in the text, while the $t_{\rm tide}^{-1}$ values are computed by comparing to the second set of simulations without dissipative terms.

Moon	Q of Saturn	$t_{\rm tide}^{-1}({\rm Gyr}^{-1})$
Radio Tracking		
Titan	124^{+26}_{-19}	0.092 ± 0.016
Astrometry		
Mimas	$25000^{+870000}_{-23000}$	0.085 ± 0.087
Enceladus	2030^{+3150}_{-1330}	0.087 ± 0.047
Tethys	7000^{+5000}_{-2200}	0.080 ± 0.042
Dione	3900^{+40100}_{-2200}	0.077 ± 0.042
Rhea	274^{+85}_{-55}	0.17 ± 0.042
Titan	61^{+240}_{-31}	0.21 ± 0.17

Supplementary Table 2: **Table of best-fit values of $Im(k_2)$ and inverse migration timescales $t_{\rm tide}^{-1}$.** Here we assume an identical value of $Im(k_2)$ and $t_{\rm tide}^{-1}$ for each moon. The reduced chi-squared values $\chi^2_{\rm red}$ are shown for each model, for each value of Enceladus's heating rate.

Enceladus heating rate	3 GW	10 GW	33 GW	55 GW
$Im(k_2)$	1.9×10^{-3}	1.7×10^{-3}	1.3×10^{-3}	1.1×10^{-3}
$\chi^2_{\rm red}$	1400	1100	610	410
$t_{\rm tide}^{-1}({\rm Gyr}^{-1})$	0.11			
$\chi^2_{\rm red}$	0.87			

Enceladus's heating rate, with the best-fit value of $Im(k_2)$ shown in Table 2. In the resonance locking model, the value of $t_{\rm tide}^{-1}$ is expected to be approximately constant. So, we perform the same fit for a constant inverse migration time, $t_{\rm tide}^{-1}$, calculated from the measured values of net migration rate as described in the Methods, with corresponding tidal migration time scale $t_{\rm tide}$ of Figure 2 in the main text. Because the second method utilizes the net migration rate, it does not depend on an assumed Enceladus heating rate. For both fits, each moon is weighted by its signal to noise, i.e., the value of $Im(k_2)$ or $t_{\rm tide}^{-1}$ divided by its uncertainty.

To quantify how well each model fits the data, we compute the reduced chi squared of each fit, $\chi^2_{\rm red}$, as shown in Table 2. The very large values of $\chi^2_{\rm red}$ for the constant Q model firmly rule it out. Moreover, it is clear that a model with a constant migration timescale is strongly preferred over a constant Q model, as the value of $\chi^2_{\rm red}$ is more than two orders of magnitude smaller for the constant migration timescale model.

Accounting for Titan's Angular Momentum Prior work[1] neglected the angular momentum (AM) of moons because they are usually very small compared to that of the planet. Titan's large mass and semi-major axis, however, means that its orbital moment of inertia is roughly 1/3 that of Saturn, and is non-negligible. To include this effect, we examine the system's total AM J,

$$\begin{aligned} J &= J_{\rm Sa} + J_{\rm Ti} \\ &\simeq I_{\rm Sa}\Omega + M_{\rm Ti}\sqrt{GM_{\rm Sa}a_{\rm Ti}}\,, \end{aligned} \tag{1}$$

where Ω is Saturn's angular rotation frequency, and $I_{\rm Sa}$ is its moment of inertia. We neglect the AM of other moons, which are negligible in comparison. Taking the time derivative of equation 1, assuming the total AM and masses are conserved, and neglecting effects of other moons, we have

$$0 = I_{\rm Sa}\dot{\Omega} + \dot{I}_{\rm Sa}\Omega + \frac{1}{2}M_{\rm Ti}\sqrt{GM_{\rm Sa}a_{\rm Ti}}\frac{\dot{a}}{a}\,. \tag{2}$$

As Saturn evolves, its moment of inertia and rotation rate will change. Defining evolutionary timescales $t_{\rm p}^{-1} = \dot{\Omega}/\Omega$, and $t_I^{-1} = \dot{I}/I$, equation 2 can be rearranged to find

$$t_{\rm p}^{-1} = -t_I^{-1} - \frac{J_{\rm Ti}}{2J_{\rm Sa}}t_{\rm tide}^{-1}\,. \tag{3}$$

The coupled planetary and orbital evolution during a resonance lock was previously derived[1], where it was found that

$$t_{\rm tide}^{-1} = \frac{2}{3}\left[\frac{\Omega}{\Omega_{\rm moon}}\left(t_\alpha^{-1} - t_{\rm p}^{-1}\right) - t_\alpha^{-1}\right], \tag{4}$$

where $t_\alpha = \omega_\alpha/\dot{\omega}_\alpha$ is the timescale on which the inertial wave or gravity mode frequency is changing, and ω_α is the wave/mode frequency measured in the rotating frame of Saturn. Inserting equation 3 into equation 4, we find

$$t_{\rm tide}^{-1} = \frac{2}{3}\left(1 - \frac{I_{\rm Ti}}{3I_{\rm Sa}}\right)^{-1}\left[\frac{\Omega}{\Omega_{\rm Ti}}\left(t_\alpha^{-1} + t_I^{-1}\right) - t_\alpha^{-1}\right]. \tag{5}$$

The value of $I_{\rm Ti}/I_{\rm Sa} \sim 1/3$, so we find that including Titan's moment of inertia only produces a $\sim 10\%$ correction to the resonance locking migration rate. Our theoretical predictions neglect this effect because it is smaller than our measurement uncertainties, and smaller than the theoretical uncertainties in parameters such as t_α and t_I.

Accounting for Coriolis forces If resonance locking occurs via a tidally excited gravity mode (g mode), Coriolis forces will affect its frequency evolution. Using the traditional approximation, the angular frequency ω and radial wavenumber k_r of a g mode are related by

$$\omega = \frac{\lambda^{1/2} N}{r k_r} \,, \tag{6}$$

where N is the Brunt-Väisälä frequency, λ is the angular eigenvalue of the g mode, and $\lambda = \ell(\ell+1)$ in the non-rotating limit. Note that in the rotating frame of Saturn, Titan's tidal forcing frequency is $\omega_{\rm force} = m(\Omega - \Omega_{\rm Ti})$, where m is the azimuthal mode number. Since $\Omega_{\rm Ti} \ll \Omega$, we have $\omega_{\rm force} \simeq m\Omega$. For $m = 2$ modes, the Coriolis parameter is $\nu = 2\Omega/\omega_{\rm force} \simeq 2/m$. We expect $m = 2$ modes are the most likely to contribute to tidal interaction, so we expect $\nu \sim 1$.

For a mode of given radial order, the value of rk_r in equation 6 is nearly constant. Taking the time derivative of equation 6, we then have

$$t_\alpha^{-1} \simeq \frac{\dot\lambda}{2\lambda} + \frac{\dot N}{N} \,. \tag{7}$$

Then using

$$\begin{aligned}
\dot\lambda &= \frac{d\lambda}{d\nu}\frac{d\nu}{dt} \\
&= \frac{d\lambda}{d\nu}\left(\frac{2\dot\Omega}{\omega_{\rm force}} - \frac{2\Omega\dot\omega_{\rm force}}{\omega_{\rm force}^2}\right) \\
&= \lambda \frac{d\ln\lambda}{d\ln\nu}\left(\frac{\dot\Omega}{\Omega} - \frac{\dot\Omega - \dot\Omega_{\rm Ti}}{\Omega - \Omega_{\rm Ti}}\right) \\
&= \lambda \frac{d\ln\lambda}{d\ln\nu}\left(\frac{-3\Omega_{\rm Ti}\Omega t_{\rm tide}^{-1} - 2\Omega_{\rm Ti}\Omega t_{\rm p}^{-1}}{\Omega(\Omega - \Omega_{\rm Ti})}\right) ,
\end{aligned} \tag{8}$$

and we have used $m = 2$. Inserting equation 8 into equation 7, and inserting that into equation 4, we find

$$t_{\rm tide}^{-1} = \frac{2}{3(1 + d\ln\lambda/2d\ln\nu)}\left[\frac{\Omega - \Omega_{\rm Ti}}{\Omega_{\rm Ti}}\frac{\dot{N}}{N} - \left(\frac{\Omega}{\Omega_{\rm Ti}} + \frac{1}{2}\frac{d\ln\lambda}{d\ln\nu}\right)t_{\rm p}^{-1}\right]. \tag{9}$$

Near $\nu \sim 1$, we expect $d\ln\lambda/d\ln\nu \sim 1$, so inclusion of Coriolis forces has a modest effect on the resonance locking dynamics of gravity modes.

Since $\Omega_{\rm Ti} \ll \Omega$, we find the resonance locking migration rate of equation 9 due to gravity modes approximately scales as

$$t_{\rm tide}^{-1} \propto \frac{\Omega}{\Omega_{\rm moon}}. \tag{10}$$

Resonance locking with g modes thus predicts *faster* migration for moons with larger semi-major axes. The observational results do not appear to show this trend, and instead it appears that $t_{\rm tide}$ is approximately constant for each of Saturn's moons. This may favor resonance locking with inertial waves, discussed below.

Resonance locking with inertial waves Following prior work[1], "resonances" with inertial waves occur near frequencies where inertial waves are focused onto attractors[2] and the energy dissipation rate is much larger. In the inertial frame, the resonance lock condition is

$$-m\Omega_{\rm moon} = (c - m)\Omega\,, \tag{11}$$

where $c < 2$ is a constant determined by the internal structure of Saturn. Note that if c remains constant as Saturn's internal structure evolves, then migration in resonance lock with inertial waves requires

$$\frac{\dot{\Omega}_{\rm moon}}{\Omega_{\rm moon}} = \frac{\dot{\Omega}}{\Omega}. \tag{12}$$

This translates to

$$t_{\rm tide}^{-1} = -\frac{2}{3}t_p^{-1}. \tag{13}$$

In this very simple model, resonantly locked moons all have *the same* migration timescale outward, regardless of their semi-major axis or mass. However, in order for resonance locking to occur, the planet's spin frequency must *decrease* with time. This is contrary to what is expected if the planet is slowly gravitationally contracting, which typically results in spin up with time.

In the more general case when c evolves with time, we have

$$\frac{\dot{\Omega}_{\rm Ti}}{\Omega_{\rm Ti}} = -\frac{\dot{c}}{m-c} + \frac{\dot{\Omega}}{\Omega}\,, \tag{14}$$

leading to

$$t_{\rm tide}^{-1} = \frac{2}{3} t_c^{-1} - \frac{2}{3} t_p^{-1}\,, \tag{15}$$

where $t_c = \dot{c}/(m-c)$.

As pointed out previously[1], in the limit of constant spin, resonance locking with inertial modes requires that t_c be positive. Since the quantity $(m-c)$ is positive for $m = 2$, this requires that $\dot{c}$ is positive, i.e., the frequency of the inertial wave attractor (as measured in the rotating frame) must be increasing. While the value of $\dot{c}/(m-c)$ depends on the internal structural evolution of Saturn, we might expect this quantity to be similar for each moon caught in a resonance lock with inertial waves. We would thus expect a similar value of $t_{\rm tide}$ for each moon, though perhaps with order unity variance. This is consistent with the observational results of the main text. Hence, we suggest that resonance locking with inertial waves (rather than g modes) is the most likely explanation for the observed moon migration rates. In this case, we do not expect to be able to detect perturbations to Saturn's gravity field due to resonantly excited gravity modes. Unfortunately, tidally excited inertial waves are not expected to be detectable either[3], because they dissipate more efficiently and hence affect Saturn's $Im(k_2)$ without substantially affecting Saturn's value of $Re(k_2)$.

Orbital Evolution of Moons Our results in Figure 2 of the main text demonstrate that Saturn's moons currently have a similar migration time scale of order $t_{\rm tide} \sim 10\,{\rm Gyr}$. Here we explore models of the long-term orbital evolution of the moons. In the resonance locking theory, the migration time scale is determined by the time scale on which the planet's structure and spin rate evolve. More detailed modeling of the coupled evolution of Saturn's interior structure, and the consequential resonance locking migration timescale, should be performed to develop reliable predictions. However, we note that planets generally evolve much faster (e.g., by cooling and contracting[4–7]) when they are young. At any given time since formation, we expect the evolution timescale of the planet (and hence the value of $t_{\rm tide}$) to be comparable to its age. Hence, we expect orbital evolution of the form

$$\frac{1}{t_{\rm tide}} = \frac{1}{a}\frac{da}{dt} \approx \frac{B}{t}\,, \tag{16}$$

where t is Saturn's age and B is a constant of order unity that is determined by the precise rate at which Saturn's inertial wave frequencies are evolving. While B is difficult to predict from first principles, Figure 2 of the main text shows that the moons all have a current migration timescale of roughly $t_{\rm tide} \sim 13\,{\rm Gyr}$, corresponding to $B \sim 1/3$, though we note B may vary slightly for different moons, and at different times.

Nonetheless, we can attempt to solve for the approximate orbital evolution of the moons. Integrating equation 16, we can solve for the orbital distance as a function of time,

$$a = a_0 \left(\frac{t}{t_0}\right)^B\,, \tag{17}$$

where a_0 and t_0 are a moon's current semi-major axis, and Saturn's current age. So, we expect the orbits to expand as a power law function of time whose exponent and normalization can be markedly different from constant Q models. Combining equation 16 with equation 1 of the

main text, we can solve for an effective tidal quality factor $Q_{\rm ef}$ as a function of orbital distance,

$$Q_{\rm ef} = \frac{3k_2}{B}\frac{G^{1/2}M_{\rm moon}R^5}{M_{\rm Sa}^{1/2}}\frac{t_0}{a_0^{1/B}}a^{-13/2+1/B}\,. \tag{18}$$

So, the effective quality factor is a sensitive function of the semi-major axis of a moon, and should not be assumed to be constant in time or space.

Figure 3 of the main text shows an example of the expected orbital evolution of Saturn's moons, using $B = 1/3$ for each moon, which predicts that each moon's orbital distance evolves as $a \propto t^{1/3}$. We do not take mean-motion resonances into account, but we note that for a constant value of B, the orbital period ratio of moons remains constant. We solve for the moon's positions from the present day back to an age of 100 Myr, before which resonance theory may start to break down. Figure 3 of the main text also shows an orbital evolution for a constant $Q = 5000$, roughly consistent with the inner moons' current orbital expansion rates. We can see that assuming a constant Q produces drastically different orbital evolution, leading to faster expansion of the inner moons' orbits and slower expansion of the outer moons' orbits.

We caution that the evolution shown in Figure 3 of the main text is a fairly crude model for the long-term evolution of Saturn's moon system. Nonetheless, we expect the resonance locking tracks to be better approximations than constant Q models. These results indicate that the semi-major axes of Rhea and Titan may have evolved by a factor of a few over the age of the solar system, orders of magnitude more than prior expectations. Figure 3 of the main text also indicates that the inner moons (Mimas, Enceladus, Tethys, and Dione) may have formed out of Saturn's rings (i.e., where the tracks cross the gray horizontal line) well after the formation of Saturn, as postulated by several recent works[8,9]. However, this result is tentative because it depends on the exact value of B for different moons and whether it evolves with time. More detailed calculations should be performed to answer this question, examining the

coupled evolution of Saturn's interior, dynamical tidal response, and moon orbital positions.

Effect on the residuals The inclusion of dissipation at Titan's frequency was necessary to fit the data (see Supplementary Figures 1 and 2). Supplementary Figure 3 shows the obtained Doppler residuals when no migration is allowed, two hours before and after the close encounter. There are remaining signatures in the vicinity of the close encounters, especially during T74. For comparison, Supplementary Figure 4 shows the obtained residuals, also two hours before and after the close encounter, when Saturn's dissipation at Titan's frequency was added to the estimated parameters. This plots evidences a better fit of the data.

1. Fuller, J., Luan, J. & Quataert, E. Resonance locking as the source of rapid tidal migration in the Jupiter and Saturn moon systems. *Mon. Not. R. Astron. Soc.* **458**, 3867–3879 (2016).

2. Ogilvie, G. I. & Lin, D. N. C. Tidal Dissipation in Rotating Giant Planets. *Astrophys. J.* **610**, 477–509 (2004).

3. Luan, J., Fuller, J. & Quataert, E. How Cassini can constrain tidal dissipation in Saturn. *Mon. Not. R. Astron. Soc.* **473**, 5002–5014 (2018).

4. Leconte, J. & Chabrier, G. Layered convection as the origin of Saturn's luminosity anomaly. *Nature Geoscience* **6**, 347–350 (2013).

5. Guillot, T. & Gautier, D. Giant Planets. *arXiv e-prints* arXiv:1405.3752 (2014). 1405.3752.

6. Fortney, J. J. *et al.* The Interior of Saturn. *arXiv e-prints* arXiv:1609.06324 (2016). 1609.06324.

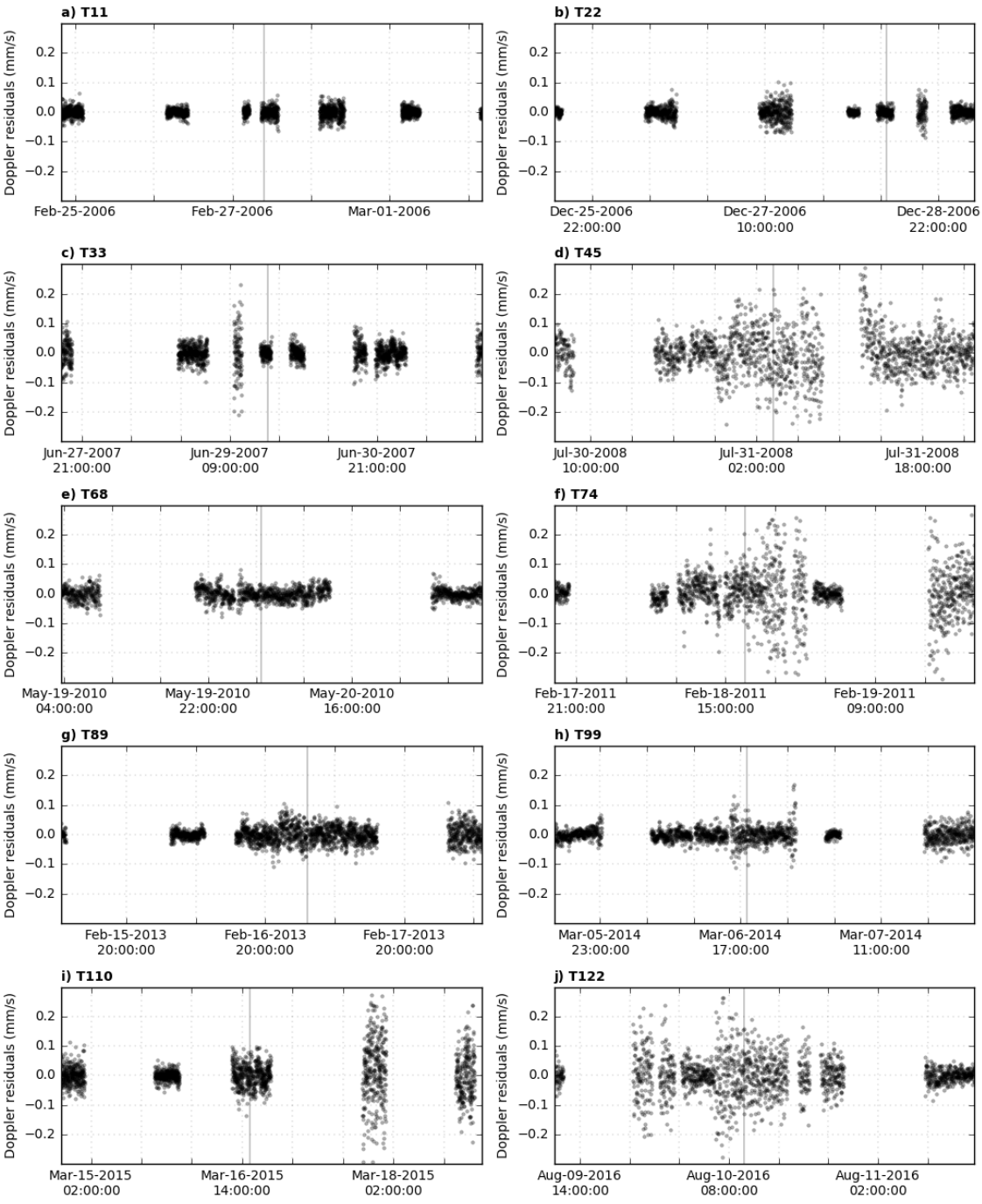

Supplementary Figure 1: **Range-rate residuals integrated over 60 s.** Panels (a-j) show the corresponding range-rate data for each arc. The vertical line corresponds to the close encounter with Titan.

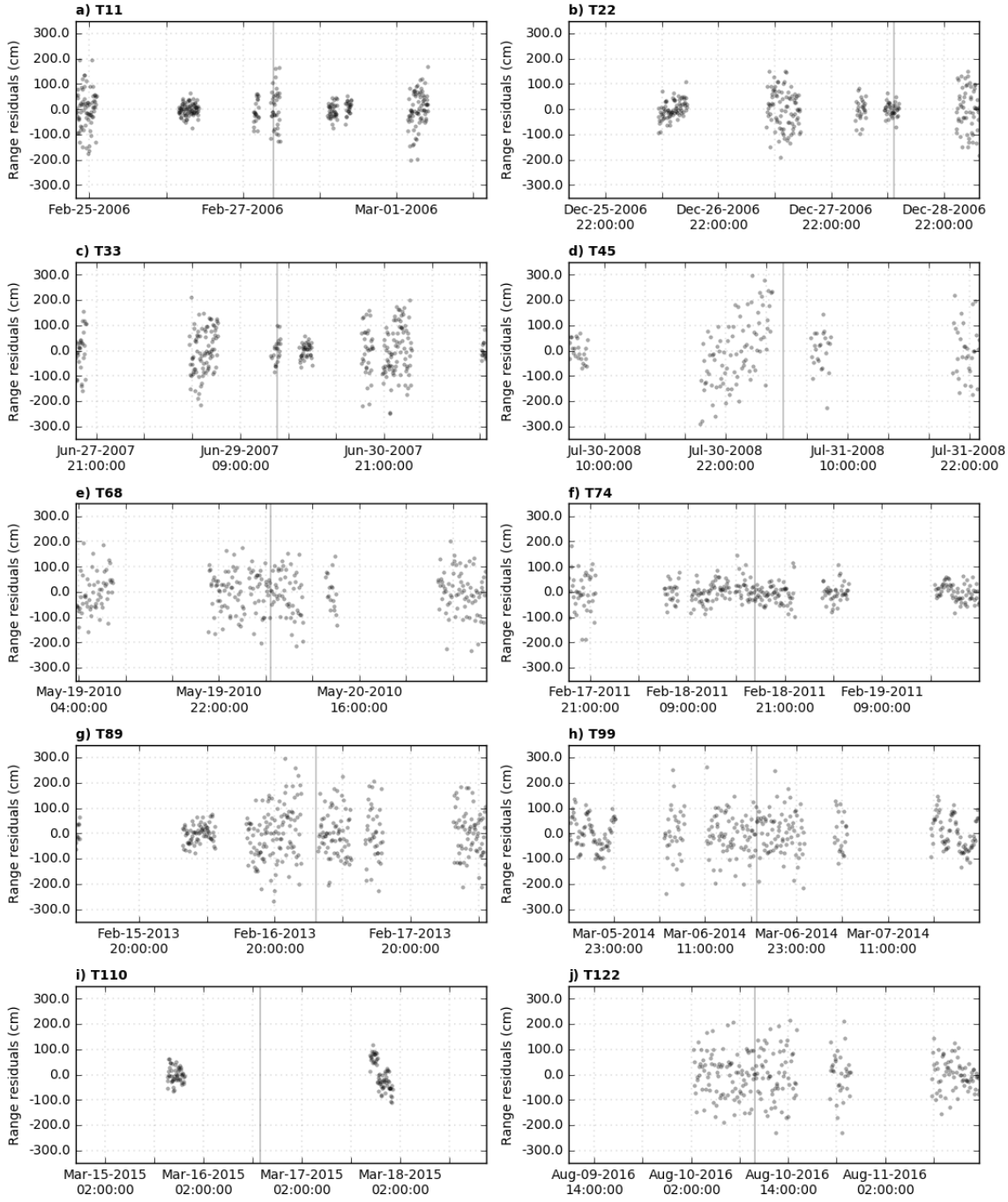

Supplementary Figure 2: **Range residuals integrated over 60 s.** Panels (a-j) show the corresponding range data for each arc. The vertical line corresponds to the close encounter with Titan.

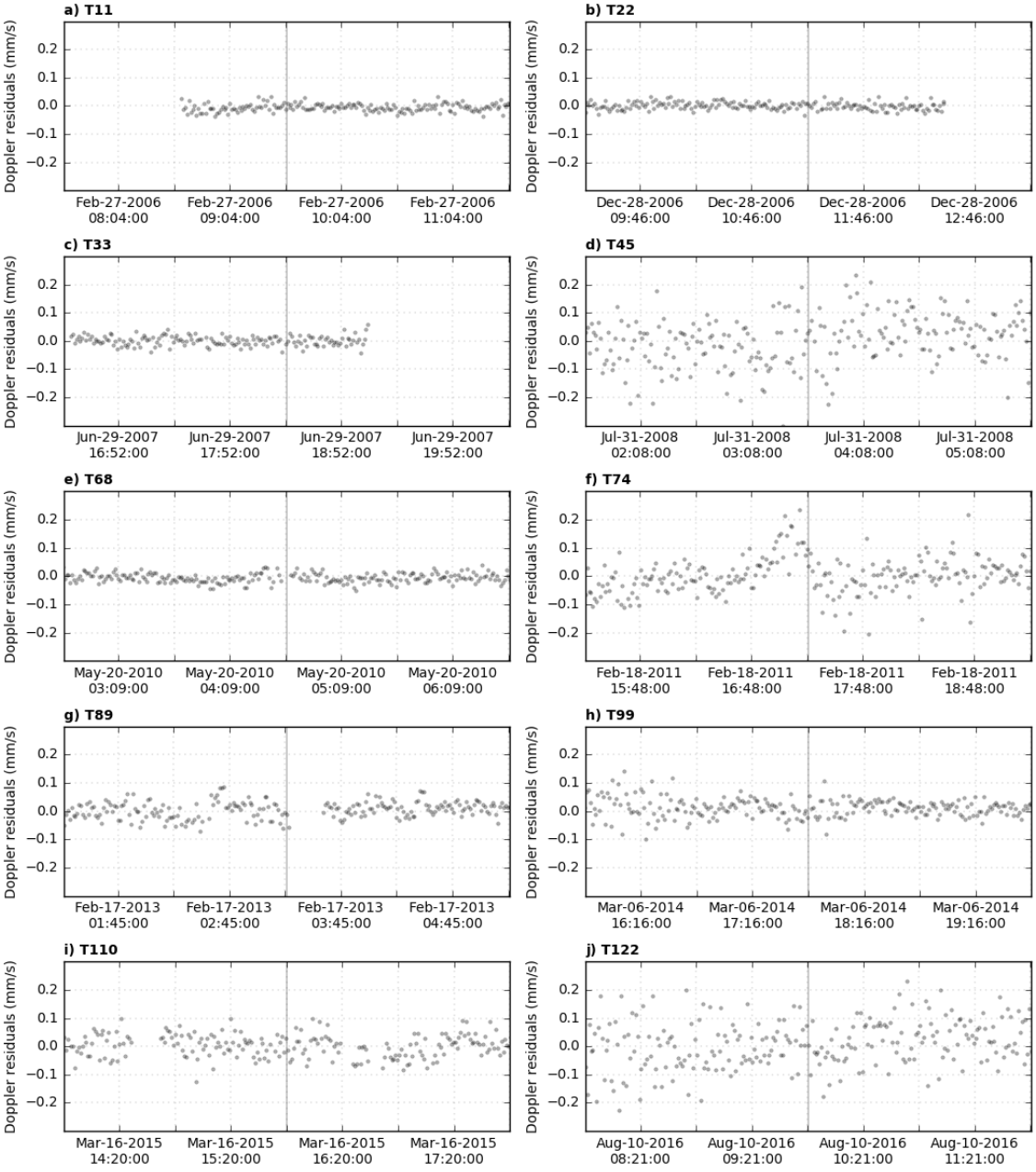

Supplementary Figure 3: **Range-rate residuals, two hours before and after the close encounter, without any tidal migration.** Panels (a-j) show the corresponding range data for each arc. The vertical line corresponds to the close encounter with Titan.

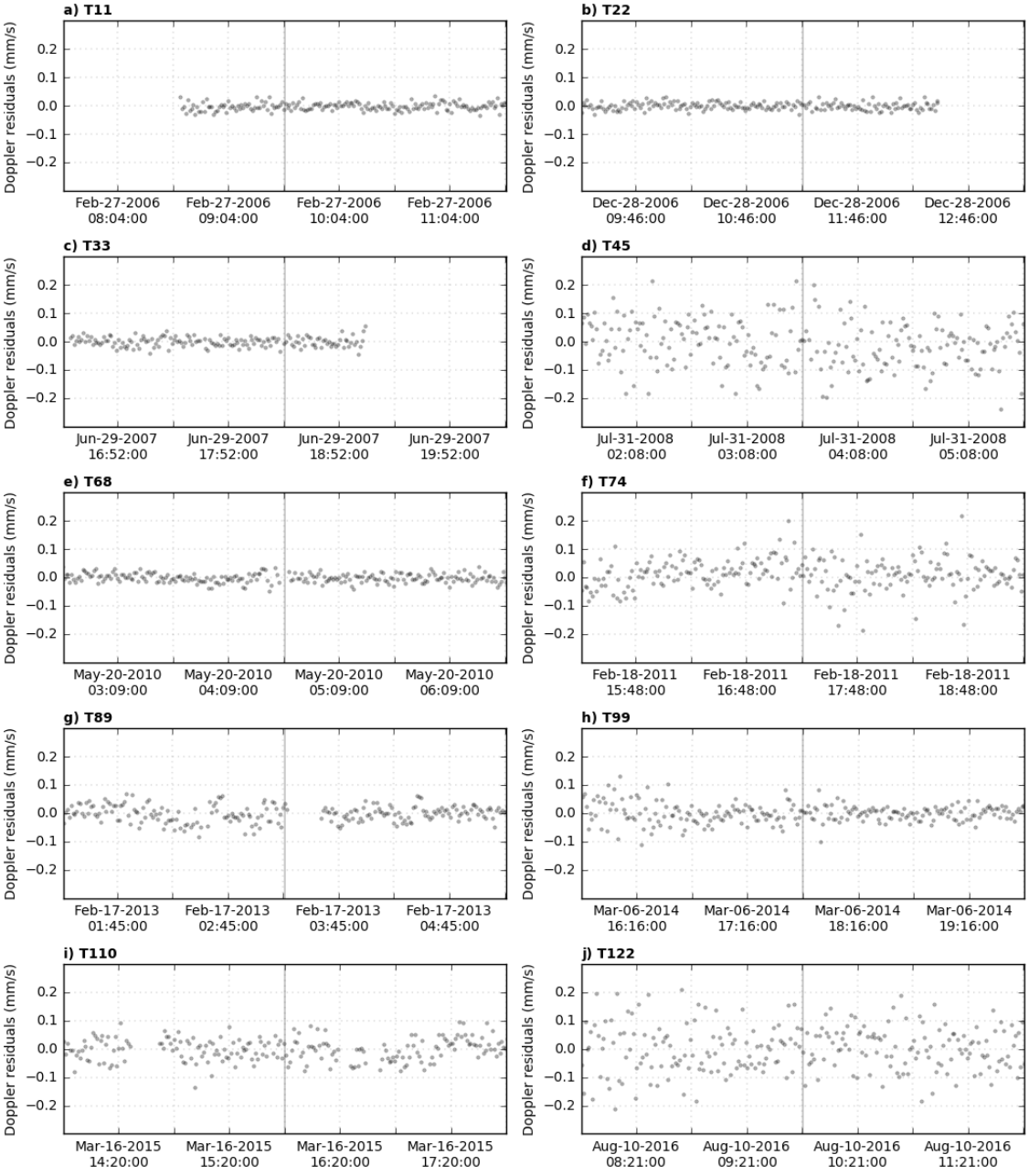

Supplementary Figure 4: **Range-rate residuals, two hours before and after the close encounter, including tidal migration.** Panels (a-j) show the corresponding range data for each arc. The vertical line corresponds to the close encounter with Titan.

7. Vazan, A., Helled, R. & Guillot, T. Jupiter's evolution with primordial composition gradients. *Astron. Astrophys.* **610**, L14 (2018).

8. Charnoz, S. *et al.* Accretion of Saturns mid-sized moons during the viscous spreading of young massive rings: Solving the paradox of silicate-poor rings versus silicate-rich moons. *Icarus* **216**, 535–550 (2011).

9. Crida, A. & Charnoz, S. Formation of Regular Satellites from Ancient Massive Rings in the Solar System. *Science* **338**, 1196– (2012).